Laser-driven production of the antihydrogen molecular ion

Mark C. Zammit,[1,*] Michael Charlton,[2] Svante Jonsell,[3] James Colgan,[1] Jeremy S. Savage,[4] Dmitry V. Fursa,[4] Alisher S. Kadyrov,[4] Igor Bray,[4] Robert C. Forrey,[5] Christopher J. Fontes,[1] Jeffery A. Leiding,[1] David P. Kilcrease,[1] Peter Hakel,[1] and Eddy Timmermans[1]

[1]*Los Alamos National Laboratory, Los Alamos, New Mexico 87545, USA*
[2]*Department of Physics, College of Science, Swansea University, Singleton Park, Swansea, SA2 8PP, United Kingdom*
[3]*Department of Physics, Stockholm University, SE-10691 Stockholm, Sweden*
[4]*Curtin Institute for Computation and Department of Physics and Astronomy, Curtin University, Perth, Western Australia 6102, Australia*
[5]*Department of Physics, Penn State University, Berks Campus, Reading, Pennsylvania 19610, USA*

(Received 9 July 2019; published 24 October 2019)

The feasibility of producing the molecular antihydrogen anion $\overline{\mathrm{H}}_2^-$ in the laboratory is investigated. Utilizing reaction rates calculated here involving the interaction of laser excited-state antihydrogen atoms held in magnetic minimum traps, key processes are identified that could lead to anion production, as well as competing effects leading to anti-atom loss. These are discussed in the context of present-day and near-future experimental capabilities.

DOI: 10.1103/PhysRevA.100.042709

I. INTRODUCTION

Recent years have seen marked progress in the production of, and experimentation with, atomic antimatter in the form of antihydrogen, $\overline{\mathrm{H}}$. Advances include controlled anti-atom creation by the merging of tailored clouds of positrons (e^+) and antiprotons ($\overline{p}$) [1,2], its capture [3,4], long-term confinement [5] and accumulation [6] in magnetic minimum neutral atom traps, and the first observations of some of the properties of $\overline{\mathrm{H}}$ [7–10], including the landmark observation of the two-photon $1s$-$2s$ transition [11], the determination of its frequency to parts in 10^{12} [12], and observation of the $\overline{\mathrm{H}}$ $1s$-$2p$ Lyman α line [13].

Very recently [12], around 10^3 $\overline{\mathrm{H}}$ were accumulated and held in the ALPHA apparatus [14] with a lifetime in excess of 60 hours. Such experiments, which take place at the Antiproton Decelerator at CERN [15,16], involve repeated cycles of $\overline{\mathrm{H}}$ formation (via $e^+ + e^+ + \overline{p} \rightarrow \overline{\mathrm{H}} + e^+$), while the anti-atoms created previously remain stored in the trap. This raises the intriguing possibility of observing reactions involving the trapped $\overline{\mathrm{H}}$, including perhaps with its constituent antiparticles, to produce more complex antimatter species. Here we discuss $\overline{\mathrm{H}}_2^-$, the bound state of two antiprotons and a positron. This ion is the antimatter counterpart of the simplest molecular system, H_2^+, which has attracted much interest over several decades from both experiment and theory (see, e.g., Refs. [17–21]) due, among other things, to its significance in astrophysics and the early Universe [22–24]. By analogy with the hydrogen-reactions work of Dalgarno and coworkers [23], we identified the manufacture of $\overline{\mathrm{H}}_2^-$ as the key gateway to produce more complex antimatter species, including neutral molecular antihydrogen and charged clusters. Furthermore, Myers [25,26] recently argued that spectroscopic investigations of the anti-anion can offer very sensitive tests of the charge parity time (CPT) theorem, which is one of the primary motivations for undertaking experiments with antimatter systems (see, e.g., Ref. [27] for a review). We note that charged species can be held virtually indefinitely in deep electromagnetic traps (see e.g., Refs. [28–30]) for future exploitation, and that a single $\overline{\mathrm{H}}_2^-$ may be sufficient to allow experimentation [25,26].

The hydrogen chemistry network has been studied extensively in its application to laboratory-produced low-temperature plasmas [31], gas clouds chemistry [32–35], and the chemistry of the early Universe [22–24,36–40]. In particular, our discussion has been motivated by the striking similarities between present-day combined antiparticle and anti-atom traps, with their very long lifetimes for all confined species [12,14], and the cosmological recombination era, where atoms were formed and the remaining ions (p, H^-), atoms (H), and free electrons (e^-) could take part in chemical reactions. During that time there was a very low abundance of molecular reactants and no dust, hence molecular ions were primarily formed via radiative association (RA),

$$\mathrm{H}(nl) + p^+ \rightarrow \mathrm{H}_2{}^+(1s\sigma_g, v, N) + \gamma(\lambda_\gamma), \tag{1}$$

associative detachment (AD),

$$p^+ + \mathrm{H}^-(nLS) \rightarrow \mathrm{H}_2{}^+(1s\sigma_g, v, N) + e^-, \tag{2}$$

and associative ionization (AI)

$$\mathrm{H}(nl) + \mathrm{H}(n'l') \rightarrow \mathrm{H}_2{}^+(1s\sigma_g, v, N) + e^-. \tag{3}$$

In nature, the density of reactants was small and processes typically involved the respective ground states, leading to relatively slow production rates of $\mathrm{H}_2{}^+$. However, in general, cross sections can be considerably enhanced by having excited reactants, which is controllable in the laboratory. This idea has

*mzammit@lanl.gov

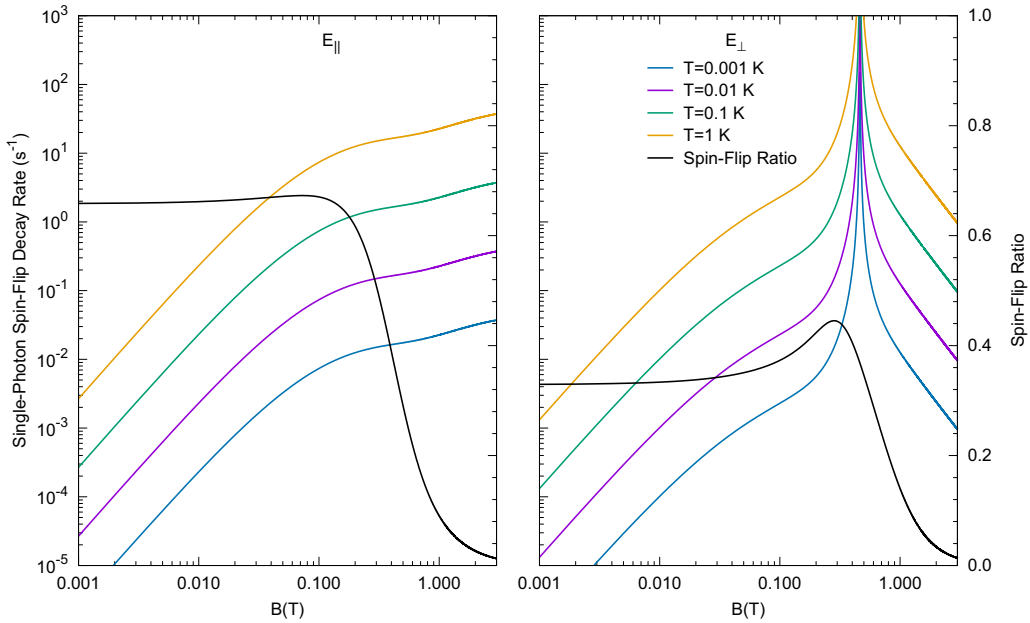

FIG. 1. The $\overline{\mathrm{H}}(2s)$ single-photon spin-flip decay rate as a function of the magnetic-field strength for selected $\overline{\mathrm{H}}$ temperatures between $T_{\overline{\mathrm{H}}} =$ 1 mK and 1 K. We take the most probable speed of the Maxwellian distribution function $v_p = \sqrt{2k_B T_{\overline{\mathrm{H}}}/m_{\overline{\mathrm{H}}}}$ (with $m_{\overline{\mathrm{H}}}$ being the antihydrogen mass) in the calculation of the electric-field strength and note that the rates are presented for the $(\mathbf{v} \times \mathbf{B})$-induced electric field parallel (left panel) or perpendicular (right panel) to the magnetic field. The spin-flip ratio is the ratio of the $2s$ single-photon spin-flipping rate and the overall $2s$ single-photon decay rate.

been investigated for the production of $\overline{\mathrm{H}}$ [41–43] and could be applicable in the antimatter case to the production of $\overline{\mathrm{H}}_2^-$. This idea is developed here.

II. METHOD

To investigate the production of $\overline{\mathrm{H}}_2^-$, we evaluate the rates for the relevant formation processes, and for those that compete for anti-atom flux, at temperatures below 1 K. We envisage a scenario in which $\overline{\mathrm{H}}$ atoms are trapped in equilibrium, possibly together with $\overline{p}$, without the presence of positrons. This means that we can ignore interactions of the H^- analog, $\overline{\mathrm{H}}^+$ (process (2)), a species with an expected very low production rate [44,45]. Furthermore, we consider that the $\overline{\mathrm{H}}$ may be laser excited, and in particular to the metastable $2s$ state [$\overline{\mathrm{H}}(2s)$] via a two-photon transition from the ground state. Thus, we consider AI interactions between pairs of excited anti-atoms, in which process (3) becomes exothermic for $(n, n' \geqslant 2)\,[\mathrm{H}(ns) + \mathrm{H}(n's)]$ reactants, and which has a relatively large cross section at low energies [46–48]. Although AI may have the largest rate coefficient for producing $\overline{\mathrm{H}}_2^-$, the competing Penning ionization (PI) process

$$\mathrm{H}(nl) + \mathrm{H}(n'l') \rightarrow p^+ + \mathrm{H}(n''l'') + e^-, \tag{4}$$

is comparable in the temperature range under consideration and can lead to depletion of the trapped $\overline{\mathrm{H}}$ sample [48]. Here we adapt the analytic fit of the AI and PI cross sections produced by Refs. [47,48] at impact energies above 10^{-4} eV, while for lower energies, we utilize the total ionization cross sections of Refs. [49,50] and the high-energy AI and PI fit [48] to determine the relative contribution of AI and PI.

We also include the specific double excitation transfer (DET) process [47,49,50]

$$\mathrm{H}(2s) + \mathrm{H}(2s) \rightarrow \mathrm{H}(2p) + \mathrm{H}(2p), \tag{5}$$

since this may lead to loss of $\overline{\mathrm{H}}$ from the trap due to spin flip deexcitation to an untrapped ground state (see below).

The magnetic fields experienced by the $\overline{\mathrm{H}}(2s)$ atoms held in a magnetic minimum trap such as that employed by ALPHA [14] cause Zeeman splitting as well as Stark-induced loss in which the $(\mathbf{v} \times \mathbf{B})$-induced electric field causes $2s$-$2p$ mixing, which can lead to $\overline{\mathrm{H}}(2s)$ single-photon decays to the ground state [51,52]. Noting that the trapped $\overline{\mathrm{H}}$ are positron spin polarized ($m_s = -1/2$), the $2s$ single-photon decays can cause a spin-flip of the positron, which leads to $\overline{\mathrm{H}}$ destruction via loss from the trap, thereby depleting the reactants available to form $\overline{\mathrm{H}}_2^-$. Utilizing the method detailed by Rasmussen *et al.* [51,52], we calculated the $\overline{\mathrm{H}}(2s)$ single-photon spin-flip decay rate as a function of the magnetic-field strength for selected $\overline{\mathrm{H}}$ temperatures between $T = 1$ mK and 1 K. These results are presented in Fig. 1, where the left and right panels correspond to the Stark-induced electric field (for the $\overline{\mathrm{H}}$ velocity) parallel and perpendicular to the magnetic field, respectively. The resonance at $B \approx 0.5$ T is due to the degeneracy of the $2s_{c/d}$ and $2p_c$ states [51,52]. These results show that, in order to reduce the destruction of $\overline{\mathrm{H}}$ via $\overline{\mathrm{H}}(2s)$ single-photon spin-flip decays, low values of $T_{\overline{\mathrm{H}}}$ and low-magnetic-field strengths are necessary.

The H_2^+ RA process has been studied for H in the ground state [53–55], and for the $\mathrm{H}(2s)$ state above an effective (assumed equilibrium) temperature of $T > 10$ K [56]. Here we calculate the RA process via excited states for $\overline{\mathrm{H}}(n \leqslant 3)$ down to $T = 1$ mK, noting that the formulation of the γ-$\overline{\mathrm{H}}_2^-$

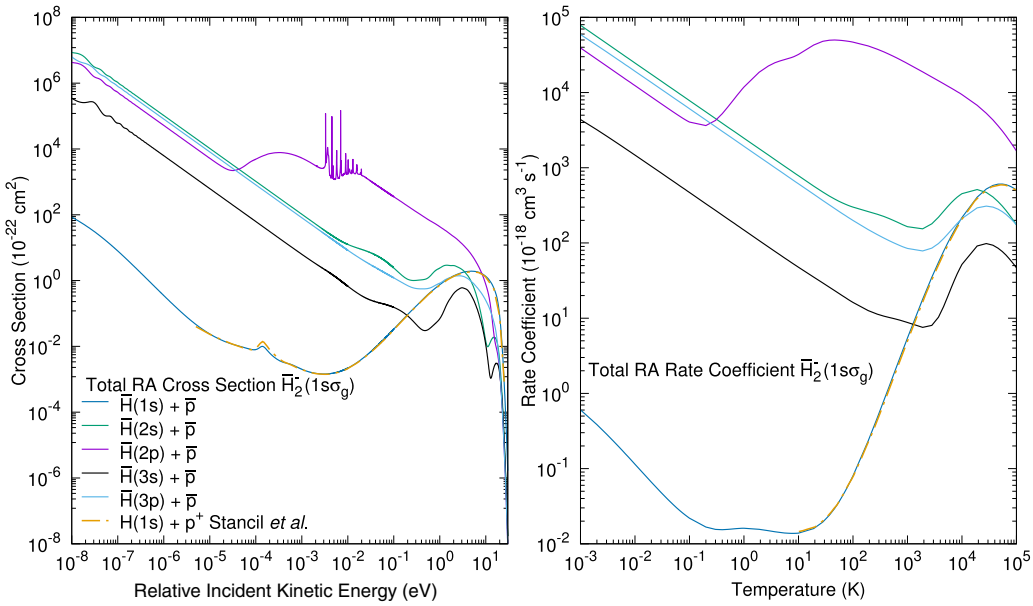

FIG. 2. The total radiative association (RA) cross section (left panel) and rate coefficient (right panel) for $\overline{H}_2^-(1s\sigma_g)$ production via the $\overline{H}(n \leqslant 3) + \overline{p}$ dipole allowed states. The present $\overline{H}(1s) + \overline{p}$ RA data are compared with those of Stancil *et al.* [53] where possible.

system is identical to that of γ-H_2^+. Here we only consider the single-photon RA process and radiative cascades will be the subject of future investigation. A detailed discussion of the method is given Ref. [56]. We note that, contrary to Ref. [56], here the total RA cross sections are calculated via an explicit sum over nuclear-spin-averaged rovibrational transitions [55].

III. RESULTS

In Fig. 2 we present the total nuclear-spin-averaged RA cross section (left panel) and rate coefficient (right panel) and compare our results for the $\overline{H}(1s) + \overline{p}$ reaction with those of Stancil *et al.* [53], showing excellent agreement where their data are available. We note that, at low energies, the RA cross section via excited state $\overline{H}$ is between 10^4–10^6 times larger than that for the $\overline{H}(1s)$ state. This dramatic difference is translated into the rate coefficient.

Figure 3 shows the $\overline{H}_2^-(1s\sigma_g)$ formation rates per cm^3 (i.e., independent of the trap interaction volume) via the RA and AI processes as a function of $\overline{H}(2s)$ density $n_{\overline{H}(2s)}$, and at selected temperatures. We also present the anti-atom removal by the PI route, the DET spin-flip decay rate, and the $2s$ single-photon spin-flip decay rates to an untrappable $\overline{H}(1s)$ state tailored, as described below, for each value of T. For the DET spin-flip decay rate we also assume that the relevant cross section has equal contributions from excitation to the so-called $2p_e$ and $2p_f$ states [51], which correspond to the two $2p_{1/2}$ level states. The RA rate for the $\overline{H}(1s)$ reaction is lower than that for the $2s$ state by a factor of 10^5–10^6, and is not given in the figure. Note that the AI and PI data are for interactions of a pair of $\overline{H}(2s)$ atoms.

It is evident from the figure that the spin-flip rate dominates, except for antihydrogen at the lowest temperature and highest densities. To reduce the loss of $\overline{H}$ via spin-flip decays low values of T and magnetic-field strength are desirable (see Fig. 1). An estimate of the magnitude of the magnetic-field difference required between the trap center at B_0 and the trap wall, to confine ground state $\overline{H}$ with a magnetic moment given by the Bohr magneton μ_B, and at a temperature T, is $\Delta B = k_B T/\mu_B \approx 1.489T$ Tesla (T) with T in units of Kelvin. Hence, as the antihydrogen ensemble temperature becomes lower, so too may the magnetic-field difference, and the absolute field strengths, needed to trap it. However, the density of a $\overline{p}$ cloud, $n_{\overline{p}}$, held in a magnetic field B_0, cannot exceed the Brillouin limit of $B_0^2\epsilon_0/2m_{\overline{p}} \approx 2.6 \times 10^9 B_0^2$ cm^{-3} (where ϵ_0 is the permittivity of free space and $m_{\overline{p}}$ is the $\overline{p}$ mass), which will affect feasible RA reaction rates when compared with those for $\overline{H}$ loss due to spin-flip decays. Furthermore, the Lorentz force from the combination of the magnetic field and the cloud radial electric field, $E_r = n_{\overline{p}} e r/2\epsilon_0$, where e is the magnitude of the elementary charge and r is the distance from the magnetic-field axis, results in a $\overline{p}$ drift speed with an effective temperature of $T_r = m_{\overline{p}} E_r^2/2k_B B_0^2 \approx 50(n_{\overline{p}} r/B_0)^2$ K, with the units of B_0, r, and $n_{\overline{p}}$ being T, mm, and 10^8 cm^{-3}, respectively.

For each value of T shown in Fig. 3 we assumed as an example that $B_0 \approx \Delta B$, from which we deduced a practical limit for $n_{\overline{p}}$ by taking $T_r = T$ and assuming $r = 0.1$ mm. It is clear that this has a marked effect on the RA rates and effectively renders this process uncompetitive if magnetic minimum traps are used to confine the anti-atom, anion formation via the AI process will be most effective in comparison with loss via spin-flip decay, which (as a worst-case scenario) we assumed the magnetic field B at the wall $B_W = B_0 + \Delta B$ for the single-photon spin-flip decay rate. This circumvents the need to produce clouds of $\overline{p}$ at mK temperatures, which is likely to be challenging.

IV. DISCUSSION

From an experimental perspective, the ALPHA group [6] produces $\overline{H}$ by using around 10^5 $\overline{p}$ at $n_{\overline{p}} \approx 3 \times 10^6$ cm^{-3} by mixing with positrons at temperatures of 15–20 K. Around 10

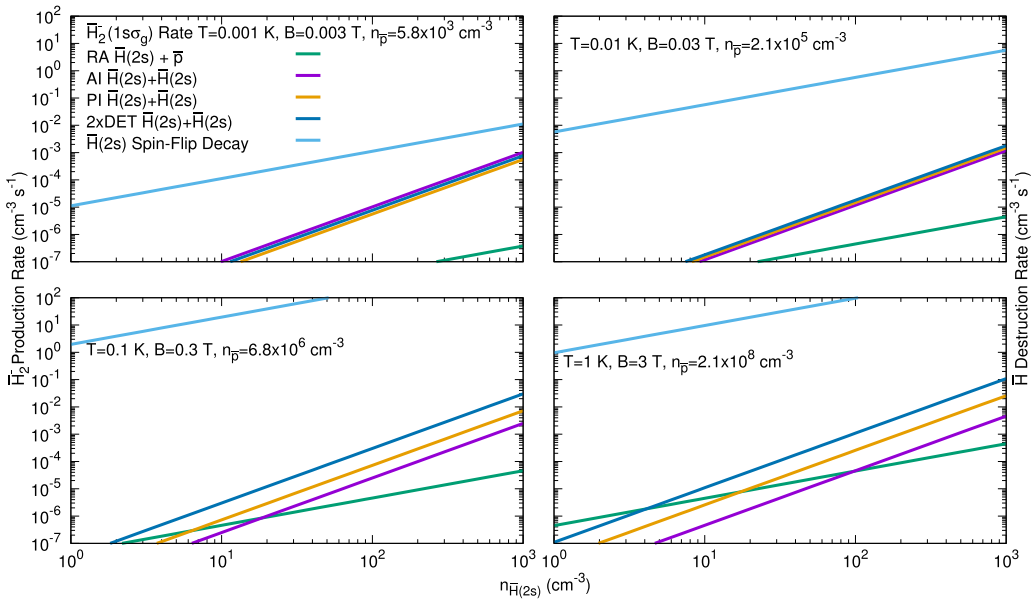

FIG. 3. The total rate per cm^3 (independent of the trap interaction volume) of $\overline{H}_2^-(1s\sigma_g)$ formation via the $\overline{H}(2s)$ reactions for selected effective temperatures between $T = 1$ mK and 1 K. We present results for radiative association (RA), associative ionization (AI), and the competing $\overline{H}$ destruction processes Penning ionization (PI), double-excitation transfer (DET) spin-flip decay, and the Stark-induced 2s single-photon spin-flip decay rate (assuming the $\overline{H}$ velocity is perpendicular to the magnetic field). The magnetic-field magnitudes B have been reduced (see text) progressively as T is lowered from 3 T at 1 K to 0.003 T at 1 mK. The resulting values of $n_{\overline{p}}$ derived by setting $T_r = T$, or by using the Brillouin limit if lower, are 2.1×10^8 cm^{-3} (1 K); 6.8×10^6 cm^{-3} (0.1 K); 2.1×10^5 cm^{-3} (0.01 K), and 5.8×10^3 cm^{-3} (0.001 K). For clarity we note for $T = 0.001$ K that the largest collision rates are from AI, DET, and PI, in that order, while for $T = 0.01$ K the largest collision rates are from DET, PI, and AI, in that order.

anti-atoms, with kinetic energies below the equivalent 0.5 K trap depth, are held each mixing cycle (of several minutes duration). The forthcoming ELENA facility at CERN [57] will provide cold $\overline{p}$ fluxes enhanced by around 10^2, and the recent accumulation of 10^3 $\overline{H}$ atoms with a lifetime in excess of two days suggests that $n_{\overline{H}}$ will be scalable with the increased $\overline{p}$ availability from ELENA. Thus, we can look forward to perhaps 10^5 or more trapped $\overline{H}$, particularly if current initiatives to produced colder positrons are successful [58]. The neutral atom trap employed by ALPHA currently has a volume of around 400 cm^3, thus $\overline{H}$ densities are just over 1 cm^{-3}, although they may approach, or exceed, 10^3 cm^{-3} in the near future. Furthermore, the recent observation of the 1s-2p $\overline{H}$ Lyman α transition [13] promises that laser cooling of $\overline{H}$ [59] into the mK region may soon be feasible.

The data presented in Fig. 3 can be converted into absolute rates by multiplying by the relevant species overlap volume, including the probability of the $\overline{H}$ being in the 2s state. We assume that the latter can approach unity for a tailored laser system, as postulated by using a Stark-chirped rapid adiabatic passage technique [60,61]. For the AI, PI, and DET processes, the overlap volume is effectively that of the entire neutral atom trap, which the long-lived 2s state can, in principle, occupy. As such $\overline{H}_2^-$ could be produced well away from the magnetic axis of the system and may not be confined due to the presence of the radial field of the antihydrogen trap [62]. We note that both the AI and PI processes will produce hot positrons; however, there will be no trapping fields present for these particles in the envisaged experiment (see below), so they will not disrupt the cold, trapped species.

A possible $\overline{H}_2^-$ production scenario is as follows: $\overline{H}$ atoms are produced, trapped, and stacked by using a similar approach to that currently used by ALPHA [6], taking advantage of advances in cooling antiparticles [58] and the increased $\overline{p}$ flux from ELENA [57], to achieve anti-atom densities of at least 10^3 cm^{-3}. Thereupon, the charged particle trapping fields can be altered to leave a shallow Penning-type arrangement for the anion. A substantial fraction of the trapped ensemble is then laser-cooled into the mK regime [6], after which the magnetic trap is lowered as far as possible in order to reduce spin-flip losses, although there will be a balance to be struck in trying to keep the cold $\overline{H}$ as close to the axis as possible to facilitate capture of any anions produced. (Anions lost by collision with the walls will have a distinctive annihilation signature, which will involve two simultaneous $\overline{p}$ events, and may be able to be isolated from the much more numerous $\overline{H}$ annihilations.) Once this is complete, the 1s-2s laser can be turned on in an effort to promote $\overline{H}_2^-$ formation via the AI route [Eq. (3)]. Formation rates for $n_{\overline{H}(2s)} = 10^3$ cm^{-3} at 1 mK are around 10^{-2} s^{-1} for an effective anion trap volume of 10 cm^3. The loss rates due to PI and DET are similar in size; however, overall loss is still dominated by spin-flip decay. The rate for the latter, given the neutral trap configuration, is likely to be around 4 s^{-1}. In the present scenario assuming all trappable $\overline{H}s$ are in the 2s state, somewhat under 4 hours of operation this scenario is approximately equivalent to $n_{\overline{H}(2s)} = 8.5 \times 10^2$ cm^{-3} and the production of 100 $\overline{H}_2^-$ (a total loss of approximately 5.8×10^4 $\overline{H}$ from the trap). Although the anion formation rate is low, we anticipate further gains as $\overline{H}$ trapping and cooling capabilities improve.

For instance, an order of magnitude increase in $n_{\overline{\mathrm{H}}(2s)}$, perhaps achieved by a reduction in the neutral trap volume, will mean that the AI and loss rates are comparable.

There has also been a suggestion to produce $\overline{\mathrm{H}}_2^-$ by the AD reaction, process (2), [25,26], by using the methodology of the GBAR experiment [63] to derive the required intermediate ion $\overline{\mathrm{H}}^+$. This approach requires the full capability of ELENA in addition to a dedicated high-flux linac-based positron beam line-plus-accumulation device to produce an average of one ion per 110 s cycle of the Antiproton Decelerator. The $\overline{\mathrm{H}}^+$ ion, which is produced at keV kinetic energies via the reaction $\overline{\mathrm{H}} + \mathrm{Ps} \rightarrow \overline{\mathrm{H}}^+ + e^-$, must then be slowed before interaction with a stored $\overline{p}$ cloud to prevent collisional breakup. Even so, losses to mutual neutralization dominate, such that only one $\overline{\mathrm{H}}^+$ ion in every 180 (with an average rate of around 5×10^{-5} s^{-1}) will result in $\overline{\mathrm{H}}_2^-$ production [25,26]. This approach is already at firm technological limits and does not appear scalable in the near future, nor seems a viable route to more complex antimatter species.

V. CONCLUSION

In summary, we have presented an analysis of possible means to produce the antihydrogen molecular anion $\overline{\mathrm{H}}_2^-$ from interactions involving trapped, excited-state antihydrogen. Although the foreseen formation rates are low, there are currently many inefficiencies in capturing, cooling, and exciting the anti-atom which provide cause for cautious optimism going forward. A more detailed study of the dynamics of $\overline{\mathrm{H}}_2^-$ formation, involving full trajectory simulations of the excited, trapped $\overline{\mathrm{H}}$ will be required to further elucidate the experimental conditions required to promote $\overline{\mathrm{H}}_2^-$ formation, detection, and capture.

ACKNOWLEDGMENTS

This work was supported by Los Alamos National Laboratory (LANL). M.C.Z. would like to specifically acknowledge LANL's ASC PEM Atomic Physics Project for its support. LANL is operated by Triad National Security, LLC, for the National Nuclear Security Administration of the U.S. Department of Energy under Contract No. 89233218NCA000001. M.C. is grateful to the EPSRC for support of his work on low-energy antimatter physics. S.J. would like to acknowledge the Swedish Research Council (VR) for financial support. J.S.S., D.V.F., I.B., and A.S.K. would like to thank the Australian Research Council for their support. R.C.F. acknowledges support from NSF Grant No. PHY-1806180.

[1] M. Amoretti *et al.* (ATHENA Collaboration), Nature (London) **419**, 456 (2002).
[2] G. Gabrielse, R. Kalra, W. S. Kolthammer, R. McConnell, P. Richerme, D. Grzonka, W. Oelert, T. Sefzick, M. Zielinski, D. W. Fitzakerley, M. C. George, E. A. Hessels, C. H. Storry, M. Weel, A. Mullers, and J. Walz (ATRAP Collaboration), Phys. Rev. Lett. **89**, 213401 (2002).
[3] G. B. Andresen *et al.* (ALPHA Collaboration), Nature (London) **468**, 673 (2010).
[4] G. Gabrielse, R. Kalra, W. S. Kolthammer, R. McConnell, P. Richerme, D. Grzonka, W. Oelert, T. Sefzick, M. Zielinski, D. W. Fitzakerley *et al.* (ATRAP Collaboration), Phys. Rev. Lett. **108**, 113002 (2012).
[5] G. B. Andresen *et al.* (ALPHA Collaboration), Nat. Phys. **7**, 558 (2011).
[6] M. Ahmadi *et al.* (ALPHA Collaboration), Nat. Commun. **8**, 681 (2017).
[7] M. Ahmadi *et al.* (ALPHA Collaboration), Nature (London) **529**, 373 (2016).
[8] C. Amole *et al.* (ALPHA Collaboration), Nat. Commun. **4**, 1785 (2013).
[9] C. Amole *et al.* (ALPHA Collaboration), Nature (London) **483**, 439 (2012).
[10] M. Ahmadi *et al.* (ALPHA Collaboration), Nature (London) **548**, 66 (2017).
[11] M. Ahmadi *et al.* (ALPHA Collaboration), Nature (London) **541**, 506 (2017).
[12] M. Ahmadi *et al.* (ALPHA Collaboration), Nature (London) **557**, 71 (2018).
[13] M. Ahmadi *et al.* (ALPHA Collaboration), Nature (London) **561**, 211 (2018).
[14] C. Amole *et al.* (ALPHA Collaboration), Nucl. Instrum. Methods Phys. Res., Sect. A **735**, 319 (2014).
[15] S. Maury, Hyperfine Interact. **109**, 43 (1997).
[16] T. Eriksson, Hyperfine Interact. **194**, 123 (2009).
[17] R. Moss, Mol. Phys. **80**, 1541 (1993).
[18] C. A. Leach and R. E. Moss, Annu. Rev. Phys. Chem. **46**, 55 (1995).
[19] L. Hilico, N. Billy, B. Grémaud, and D. Delande, Eur. Phys. J. D **12**, 449 (2000).
[20] A. D. J. Critchley, A. N. Hughes, and I. R. McNab, Phys. Rev. Lett. **86**, 1725 (2001).
[21] J.-P. Karr, F. Bielsa, A. Douillet, J. Pedregosa Gutierrez, V. I. Korobov, and L. Hilico, Phys. Rev. A **77**, 063410 (2008).
[22] D. Galli and F. Palla, Astron. Astrophys. **335**, 403 (1998).
[23] S. Lepp, P. C. Stancil, and A. Dalgarno, J. Phys. B: At., Mol. Opt. Phys. **35**, R57 (2002).
[24] C. M. Coppola, D. Galli, F. Palla, S. Longo, and J. Chluba, Mon. Not. R. Astron. Soc. **434**, 144 (2013).
[25] E. G. Myers, Phys. Rev. A **98**, 010101(R) (2018).
[26] E. G. Myers, Hyperfine Interact. **239**, 43 (2018).
[27] M. H. Holzscheiter, M. Charlton, and M. M. Nieto, Phys. Rep. **402**, 1 (2004).
[28] G. Gabrielse, X. Fei, L. A. Orozco, R. L. Tjoelker, J. Haas, H. Kalinowsky, T. A. Trainor, and W. Kells, Phys. Rev. Lett. **65**, 1317 (1990).
[29] H. Dehmelt, Phys. Scr. **T59**, 423 (1995).
[30] C. Smorra *et al.* (BASE Collaboration), Nature (London) **550**, 371 (2017).
[31] R. Janev, D. Reiter, and U. Samm (2003), Collision processes in low-temperature hydrogen plasmas, http://www.eirene.de/report_4105.pdf.

[32] G. J. Ferland, R. L. Porter, P. A. M. van Hoof, R. J. R. Williams, N. P. Abel, M. L. Lykins, G. Shaw, W. J. Henney, and P. C. Stancil, Rev. Mex. Astron. Astrofis **49**, 137 (2013).
[33] M. L. Lykins, G. J. Ferland, R. Kisielius, M. Chatzikos, R. L. Porter, P. A. M. van Hoof, R. J. R. Williams, F. P. Keenan, and P. C. Stancil, Astrophys. J. Lett. **807**, 118 (2015).
[34] K. Sugimura, C. M. Coppola, K. Omukai, D. Galli, and F. Palla, Mon. Not. R. Astron. Soc. **456**, 270 (2016).
[35] C. M. Coppola, G. Mizzi, D. Bruno, F. Esposito, D. Galli, F. Palla, and S. Longo, Mon. Not. R. Astron. Soc. **457**, 3732 (2016).
[36] P. C. Stancil, S. Lepp, and A. Dalgarno, Astrophys. J. **509**, 1 (1998).
[37] C. M. Hirata and N. Padmanabhan, Mon. Not. R. Astron. Soc. **372**, 1175 (2006).
[38] C. M. Coppola, S. Longo, M. Capitelli, F. Palla, and D. Galli, Astrophys. J., Suppl. Ser. **193**, 7 (2011).
[39] S. Longo, C. M. Coppola, D. Galli, F. Palla, and M. Capitelli, Rend. Fis. Acc. Lincei **22**, 119 (2011).
[40] C. D. Gay, P. C. Stancil, S. Lepp, and A. Dalgarno, Astrophys. J. **737**, 44 (2011).
[41] A. S. Kadyrov, C. M. Rawlins, A. T. Stelbovics, I. Bray, and M. Charlton, Phys. Rev. Lett. **114**, 183201 (2015).
[42] C. M. Rawlins, A. S. Kadyrov, A. T. Stelbovics, I. Bray, and M. Charlton, Phys. Rev. A **93**, 012709 (2016).
[43] A. S. Kadyrov, I. Bray, M. Charlton, and I. I. Fabrikant, Nat. Commun. **8**, 1544 (2017).
[44] C. M. Keating, M. Charlton, and J. C. Straton, J. Phys. B: At., Mol. Opt. Phys. **47**, 225202 (2014).
[45] B. M. McLaughlin, P. C. Stancil, H. R. Sadeghpour, and R. C. Forrey, J. Phys. B: At., Mol. Opt. Phys. **50**, 114001 (2017).
[46] X. Urbain, A. Cornet, and J. Jureta, J. Phys. B: At., Mol. Opt. Phys. **25**, L189 (1992).
[47] R. C. Forrey, R. Côté, A. Dalgarno, S. Jonsell, A. Saenz, and P. Froelich, Phys. Rev. Lett. **85**, 4245 (2000).
[48] A. Bohr, A. Blickle, S. Paolini, L. Ohlinger, and R. C. Forrey, Phys. Rev. A **85**, 042710 (2012).
[49] R. C. Forrey, S. Jonsell, A. Saenz, P. Froelich, and A. Dalgarno, Phys. Rev. A **67**, 040701(R) (2003).
[50] S. Jonsell, R. C. Forrey, A. Saenz, P. Froelich, and A. Dalgarno, Phys. Scr. **T110**, 299 (2004).
[51] C. O. Rasmussen, N. Madsen, and F. Robicheaux, J. Phys. B: At., Mol. Opt. Phys. **50**, 184002 (2017).
[52] C. O. Rasmussen, N. Madsen, and F. Robicheaux, J. Phys. B: At., Mol. Opt. Phys. **51**, 099501 (2018).
[53] P. C. Stancil, J. F. Babb, and A. Dalgarno, Astrophys. J. **414**, 672 (1993).
[54] J. F. Babb, Astrophys. J., Suppl. Ser. **216**, 21 (2015).
[55] M. Beyer and F. Merkt, Phys. Rev. X **8**, 031085 (2018).
[56] M. C. Zammit, J. S. Savage, J. Colgan, D. V. Fursa, D. P. Kilcrease, I. Bray, C. J. Fontes, P. Hakel, and E. Timmermans, Astrophys. J. Lett. **851**, 64 (2017).
[57] S. Maury, W. Oelert, W. Bartmann, P. Belochitskii, H. Breuker, F. Butin, C. Carli, T. Eriksson, S. Pasinelli, and G. Tranquille, Hyperfine Interact. **229**, 105 (2014).
[58] N. Madsen, F. Robicheaux, and S. Jonsell, New J. Phys. **16**, 063046 (2014).
[59] P. H. Donnan, M. C. Fujiwara, and F. Robicheaux, J. Phys. B: At., Mol. Opt. Phys. **46**, 025302 (2013).
[60] L. P. Yatsenko, B. W. Shore, T. Halfmann, K. Bergmann, and A. Vardi, Phys. Rev. A **60**, R4237(R) (1999).
[61] L. P. Yatsenko, V. I. Romanenko, B. W. Shore, T. Halfmann, and K. Bergmann, Phys. Rev. A **71**, 033418 (2005).
[62] J. Fajans, N. Madsen, and F. Robicheaux, Phys. Plasmas **15**, 032108 (2008).
[63] P. Pérez *et al.* (GBAR Collaboration), Hyperfine Interact. **233**, 21 (2015).